

Controlling distant contacts to reduce disease spreading on disordered complex networks

Ignacio A. Perez*

*Instituto de Investigaciones Físicas de Mar del Plata (IFIMAR)-Departamento de Física,
FCEyN, Universidad Nacional de Mar del Plata-CONICET,
Funes 3350, (7600) Mar del Plata, Argentina.*

Paul A. Trunfio

*Physics Department and Center for Polymer Studies,
Boston University, Boston, Massachusetts 02215, USA*

Cristian E. La Rocca and Lidia A. Braunstein

*Instituto de Investigaciones Físicas de Mar del Plata (IFIMAR)-Departamento de Física,
FCEyN, Universidad Nacional de Mar del Plata-CONICET,
Funes 3350, (7600) Mar del Plata, Argentina. and
Physics Department and Center for Polymer Studies,
Boston University, Boston, Massachusetts 02215, USA*

Abstract

Disorder is a characteristic of real social networks generated by heterogeneity in person-to-person interactions. This property affects the way a disease spreads through a population, reaches a tipping point in the fraction of infected individuals, and becomes an epidemic. Disorder is usually associated with contact times between individuals, and normalized contact time values ω are taken from the distribution $P(\omega) = 1/(a\omega)$ that mimics “face-to-face” experiments [1, 2]. To model more realistic systems, we study how heterogeneity in person-to-person interactions affects the spreading of diseases when two different kinds of disorder are present, each with a particular value of a . This allows two different types of interaction to emerge, such as close (family, coworkers) and distant (neighbors, strangers) contacts. We also develop a strategy for controlling distant contact times, which are easier to alter in practice, so as to reduce the total number of infected individuals. Finally, we use “face-to-face” experiments to generate a more accurate distribution of normalized contact times, and we repeat the analysis for this distribution.

Keywords: Complex network, Epidemic modelling, Percolation, SIR model

* ignauper@gmail.com

I. INTRODUCTION

Changes in social contact patterns, in recent centuries, have caused infectious diseases to propagate more rapidly and become more widespread [3]. The population growth in urban zones and the increasing speed and efficiency of air travel have allowed diseases to spread over long distances within months or even weeks. Examples include the 1918 Spanish flu [4], the 2009 A(H1N1) influenza epidemic [5], the 2014 Ebola epidemic [6], and the recent measles outbreak in Israel that propagated to New York [7]. A lot of research indicates that due to the increased resistance of bacteria to drugs [8], climate change [9, 10] and the deforestation of sylvan areas [11], the number of diseases will continue to increase. In this context, mathematical models allow epidemiologists and sanitary authorities to understand propagation processes, predict their effect on healthy populations, and evaluate the effectiveness of different mitigation and prevention strategies.

Although many models consider full mixing, in which all individuals in a population interact with each other [3], this assumption overestimates disease virulence. In recent decades, researchers have begun to model epidemic processes using complex networks, in which a node (an individual) has a probability $P(k)$ of being connected with k different nodes (neighbors) with $k_{\min} \leq k \leq k_{\max}$, where k_{\min} and k_{\max} are the minimum and maximum connectivity, respectively. Researchers have found that connection patterns strongly affect the spreading of a disease [12–17].

The susceptible-infected-recovered (SIR) model [3, 12, 13, 18] is a simple representation of non-recurrent diseases, where individuals acquire permanent immunity once they stop being ill. Examples include influenza A(N1H1), measles, and pertussis. In this model, an individual is either (1) susceptible (able to be infected), (2) infected (can propagate the disease), or (3) recovered (has either acquired immunity or died, and no longer propagates the disease). In the discrete-time Reed-Frost model [19], at each time step, infected individuals spread the disease to susceptible neighbors, with a probability β , and recover after t_r time steps since they were infected. The effective probability of infection is thus given by the transmissibility $T = 1 - (1 - \beta)^{t_r}$. The process ends when there are no more infected individuals; the system has reached the steady state. In the SIR model, at the steady state, the fraction R of recovered individuals exhibits a second-order phase transition as a function of the transmissibility T . The order parameter of the transition is R , while T is the control

parameter. Below a critical threshold $T = T_c$, the disease reaches only a small fraction of the population, but when $T > T_c$ it becomes an epidemic [12, 20–22]. Research has shown that the steady state of the SIR model is related to link percolation [12, 18, 21, 23], in which links are occupied with a probability p . This is because the disease propagating through a link, from an infected to a susceptible individual, is equivalent to occupying that link via link percolation (i.e., $T \equiv p$). Above a critical threshold $p = p_c$, a giant component (GC) of the same order of magnitude than the system size N emerges, whereas below p_c there are only finite clusters. The fraction P_∞ of nodes belonging to the GC is the order parameter of a second-order phase transition, and it was found that R in the SIR model, at the steady state, maps into P_∞ [12]. Because SIR only produces one cluster of nodes (those reached by the disease) and neglect realizations with $R < s_c$ for the mapping to exist [22]. For complex networks $p_c = 1/(\kappa - 1) = T_c$ in which $\kappa = \langle k^2 \rangle / \langle k \rangle$, $\langle k \rangle$ and $\langle k^2 \rangle$ are the first and second moments of the distribution $P(k)$, respectively [12, 18, 21].

Different strategies have been proposed for containing the spreading of diseases. Although one of the most studied, vaccination, is highly efficient in providing immunity [24–26], vaccines are often expensive and not always available for new strains. Thus, non-pharmacological strategies are needed to protect populations, particularly when an increasing number of individuals refuse available vaccines for themselves and their children. Quarantine is one of the most effective strategies to limit epidemics, but complete isolation has a negative impact on the economy of a region, and it is difficult to implement in a large population. Thus, “social distancing” [27–31] is often implemented, i.e., the interactions or the contact times between individuals are shortened. This can be carried out, for instance, by partial closure of schools and offices, and restriction of travel. For example, the government of Australia used this kind of strategy during the 2009 influenza A(H1N1) epidemic [32].

One way to studying social distancing strategies is to examine the heterogeneity in the contact times between individuals. Most research that uses the SIR model assumes that the infection probability is unique, i.e., that all individuals interact with each other in the same way. This has been contradicted by several experiments on real social networks [1, 2, 33]. For example, “face-to-face” experiments have shown that, in some cases, the contact times between individuals follow a power-law distribution [1, 2]. This heterogeneity (“disorder”) in the interactions is modeled using weighted complex networks, in which weights depend on the normalized contact times ω of the interactions. Previous SIR model research on weighted

complex networks [29, 34], takes values for ω from a theoretical power law distribution, with broadness a , that mimics the results of “face-to-face” experiments [1, 2]. The larger the parameter a , the shorter the contact times. Among other things, they found that the spreading of diseases is delayed as the broadness a increases [29]. This allows sanitary authorities to intervene earlier, thus, mitigating the impact of the disease on the population [34].

In this manuscript we analyze a social distancing strategy for halting the spreading of diseases in a more realistic scenario, modeled by weighted complex networks in which individuals can have different kinds of interactions between them. These include relationships such as close contacts (family, friends, or coworkers), and distant contacts (neighbors and contacts in public spaces, e.g., transport and commerce). To distinguish each kind of interaction, we assign them different contact time distributions, taken from “face-to-face” experiments [1, 2] and the research [29, 34] described previously. In addition, we explore a strategy for reducing the impact of diseases by modifying only distant contacts, which can be easier to manipulate.

II. MODEL AND SIMULATIONS

We construct complex networks of N nodes as a substrate for the propagation of a disease, by using the Molloy-Reed algorithm [35]. We build two types of networks with different degree distributions. First, $P(k) = e^{-\langle k \rangle} \langle k \rangle^k / k!$ —an Erdős-Rényi network (ER)—in which $\langle k \rangle$ is the average number of neighbors of each node, and second, $P(k) = Ck^{-\lambda} e^{-k/k_c}$ —a scale free network (SF)—with exponential cutoff k_c and normalization constant C . ER networks are homogeneous because their nodes have a number of neighbors mostly around the mean value of the distribution, whereas SF networks are heterogeneous and hence nodes have a greater amplitude in their connectivities, with many nodes of low connectivity and only a few nodes of high connectivity (hubs).

We use the SIR model described in Sec. I to simulate the spreading of the disease, but we assume that the infection probability is related to the contact times between individuals, i.e., the more time a susceptible individual spends with an infected person, the higher the probability they will also become infected. Thus, the infection probability is $\beta\omega$, where β is fixed and represents the intrinsic virulence of the disease and ω is the normalized contact

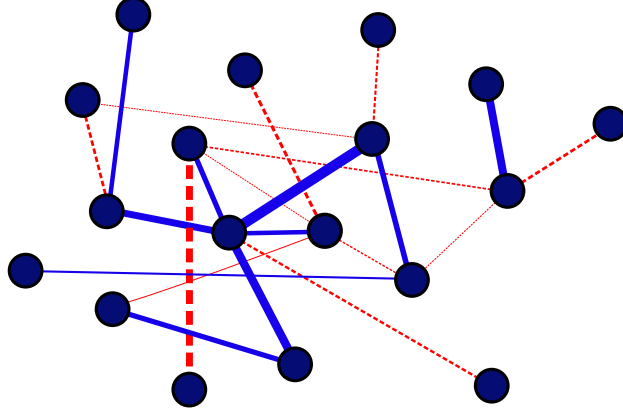


FIG. 1: Schematic of the network constructed. The different widths of the segments represent the heterogeneity of the normalized contact times ω between individuals. Contact times belonging to the fraction f_1 (—), with $a_1 < a_2$, are usually longer than those belonging to the complementary fraction $f_2 = 1 - f_1$ (---).

time between individuals. We also assume that the contact times are heterogeneous and hence we use a weighted network, in which links are characterized by weights $\beta\omega$. As in “face-to-face” experiments [1], in which contact times follow a power law distribution, we take ω from a theoretical distribution of contact times $P(\omega) = 1/a\omega$, where $\omega \in [e^{-a}, 1]$ [29, 34]. The parameter a is the *disorder intensity* and controls the width of the distribution. For fixed a , we set $\omega = e^{-ar}$, where r is randomly selected from a uniform distribution over the interval $[0, 1]$ [36]. We also separate the contacts (links) into two complementary parts, (i) a fraction f_1 of links with a distribution of contact times with disorder intensity a_1 and (ii) a fraction $f_2 = 1 - f_1$ with a distribution with disorder intensity a_2 , for $0 < f_1 < 1$. In Fig. 1 we show the fraction f_1 of interactions corresponding to the distribution with disorder intensity a_1 , $a_1 < a_2$ (blue continuous lines). On average, the interactions corresponding to the fraction f_1 have longer contact times than the ones corresponding to the fraction $f_2 = 1 - f_1$ (red dashed lines), indicated by the width of the segments. This allows a more realistic representation of populations in which different kinds of interactions can emerge. For example, when $a_1 < a_2$ we can distinguish between close and distant contacts, where a_1 and a_2 are the distribution disorders of close contacts (longer contact times) and distant contacts (shorter contact times), respectively. Because in practice the distant contacts are easier to control, our mitigation strategy focuses on modifying them to reduce the scope of the disease. In Sec. III we apply ourselves to this task.

When the propagation starts at $t = 0$, all individuals are susceptible except for one randomly-infected *patient zero*. With probability $\beta\omega$, at each time step, infected individuals propagate the disease to their susceptible neighbors, where ω is initially fixed and depends on the interaction between individuals. Each infected individual recovers after a time t_r since it was infected. The spreading process ends when there are no more infected individuals, and all are either susceptible or recovered. At this steady state the fraction R of recovered individuals for a given value of the transmissibility T indicates the extent of the disease, since all recovered individuals were previously infected.

Introducing disorder in the contact times changes the transmissibility formula [34]. In our model we must account for the densities f_1 or $1 - f_1$ of links that have weights ω corresponding to the distribution with a disorder intensity of a_1 or a_2 , respectively. Then the transmissibility T_{a_1, a_2} for a given virulence β and recovery time t_r is

$$T = T_{a_1, a_2} = f_1 T_{a_1} + (1 - f_1) T_{a_2}, \quad (1)$$

where

$$T_{a_i} = \sum_{t=1}^{t_r} \frac{(1 - \beta e^{-a_i t})^t - (1 - \beta)^t}{a_i t} \quad (2)$$

is the transmissibility of a disease in a network with a unique distribution of contact times ($f_1 = 0$ or $f_1 = 1$), with disorder intensity a_i , $i = 1, 2$ [34]. Note that the transmissibility T_{a_1, a_2} is a decreasing function of the intensities a_1 and a_2 , because for higher values of a_1 or a_2 the range of values for ω allowed in each distribution of disorder expands, and shorter contact times become more probable. Thus, the disease is less likely to propagate. On the other hand, in the limit $a_1 \rightarrow 0$ and $a_2 \rightarrow 0$ there is no disorder, and we recover the original (homogeneous) SIR model as $T_{a_1, a_2} \rightarrow T = 1 - (1 - \beta)^{t_r}$.

When carrying out the simulations we select, for the non-disorder case, an infection probability β from the epidemic phase, i.e., $\beta > \beta_c$ or $T > T_c$. Then, we determine whether there are any pair of disorder intensities (a_1, a_2) for which there is no epidemic. In Fig. 2 we show the fraction R of recovered individuals as a function of the disorder a_2 , for an ER network with $\langle k \rangle = 4$ and different values of β , where we fix $t_r = 1$, $f_1 = 0.2$ and $a_1 = 1$. We can see that for both values of β , there is a critical value a_{2c} above which the system is in a non-epidemic phase. Note that even though we have chosen a value of β for the epidemic regime without disorder in the network, the implementation of disorder reduces the spreading of the disease in the population and we obtain a non-epidemic regime. In

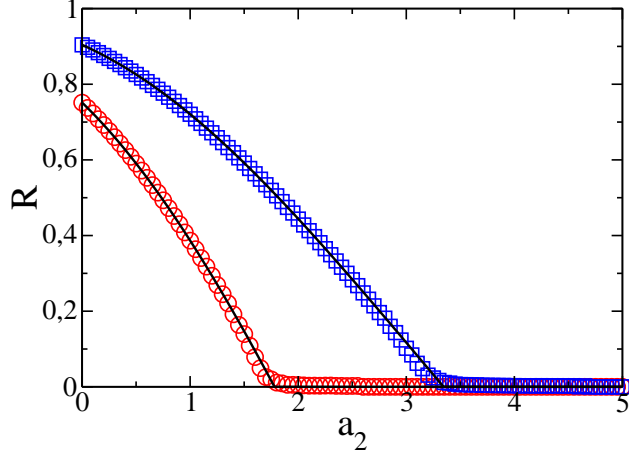


FIG. 2: Fraction R of recovered individuals at the stationary state, as a function of the disorder intensity a_2 , for $\beta = 0.5$ (\circ) and $\beta = 0.7$ (\square). Note that for each value of β there is a critical value a_{2c} , such that the system is in a non-epidemic phase for $a_2 > a_{2c}$. The results of the simulations correspond to an ER network with $k_{\min} = 0$, $k_{\max} = 40$ and $\langle k \rangle = 4$, where $f_1 = 0.2$ and $a_1 = 1$. The network size is $N = 10^5$ and the results are averaged over 10^5 realizations. The black curves (—) correspond to the theoretical results.

Sec. III we describe how to obtain the critical value for the disorder intensity a_2 and the conditions for its existence.

III. THEORY

Using the branching process formalism [12, 17, 36–38] we define the generating function of the distribution $P(k)$, $G_0(x) = \sum_k P(k)x^k$, and the generating function of the excess degree distribution $G_1(x) = \sum_k [kP(k)/\langle k \rangle]x^{k-1}$. In Fig. 2 we show the theoretical results for the fraction R of recovered individuals (black curves), obtained by solving the link percolation equations $f_\infty = 1 - G_1(1 - pf_\infty)$ and $P_\infty(p) = 1 - G_0(1 - pf_\infty)$, where f_∞ is the probability that a branch of links expands infinitely, P_∞ is the fraction of nodes in the GC, and p is the fraction of links occupied on the network. As we stated before, the SIR model can be mapped into link percolation [12, 17, 36–38], thus, R and P_∞ are equivalent. In Fig. 2 we see that the simulation results from the SIR model with disorder present an excellent agreement with the percolation theory. The previous equations and the mapping between R and P_∞ apply in the thermodynamic limit $N \rightarrow \infty$, and for locally tree-like networks.

As stated in Sec. II, our goal is to study a mitigation strategy for a population with both close and distant interactions, in which we curtail the spreading of diseases by controlling the distant contacts. If a_1 is the disorder intensity corresponding to the distribution of close contacts and a_2 corresponds to distant contacts, then $a_1 < a_2$. Next, we use the theoretical result from the mapping that sets an equivalence between T_{a_1, a_2} and p to analyze the phase space of the system, which allows us to examine our proposed mitigation strategy. In Eq. (1) we can use the critical transmissibility $T_{a_1, a_{2c}} \equiv p_c = 1/(\kappa - 1)$ to find, for $t_r = 1$,

$$\frac{1}{\kappa - 1} = f_1 \beta \frac{1 - e^{-a_1}}{a_1} + (1 - f_1) \beta \frac{1 - e^{-a_{2c}}}{a_{2c}}, \quad (3)$$

from which we can compute the critical intensity a_{2c} for different values of a_1 . In Fig. 3 we show the phase diagram on the plane (a_1, a_2) for different values of f_1 and β . Because we study close and distant contacts, our interest is focused in the region of the phase space above the dashed-dotted line, which corresponds to networks such that $a_1 < a_2$.

Each curve in Fig. 3 indicates the critical value a_{2c} as a function of a_1 for a given density f_1 . The curves separate the epidemic phase (below) from the epidemic-free phase (on and above). We also can see that in (a) there is a point $a_2^* = a_1^* = a_c$ at which all the curves cross each other for different f_1 values, where a_c is the critical intensity for a network with a unique disorder distribution. Starting from the $a_2^* = a_1^* = a_c$ point and moving away, the critical intensity a_{2c} increases as a_1 decreases. This indicates that the longer the close contact times, the shorter the distant contact times needed to avoid the epidemic phase. In Fig. 3(b) we show that a_1 can even go to zero, which means that the close contact times can be as long as possible. In this limit we see that a_{2c} converges to a finite value \tilde{a}_2 . Using Eq. (3) we obtain an expression for \tilde{a}_2 ,

$$T_c = f_1 \beta + (1 - f_1) \beta \frac{1 - e^{-\tilde{a}_2}}{\tilde{a}_2}. \quad (4)$$

Using Eq. (4) we find that \tilde{a}_2 exists if $f_1 \beta < T_c$, otherwise the close contacts cause the system to be in an epidemic phase for any value of a_2 , which means that \tilde{a}_2 does not exist. In this case, when $f_1 \beta > T_c$, $a_{2c} \rightarrow \infty$ as $a_1 \rightarrow a_{1m}$ [see Eq. (3)]. Thus, distant contact times are equal to zero, and because the disease cannot pass through these contacts its corresponding transmissibility is also zero. The resulting expression for $a_1 = a_{1m}$ is then

$$T_c = f_1 \beta \frac{1 - e^{-a_{1m}}}{a_{1m}}. \quad (5)$$

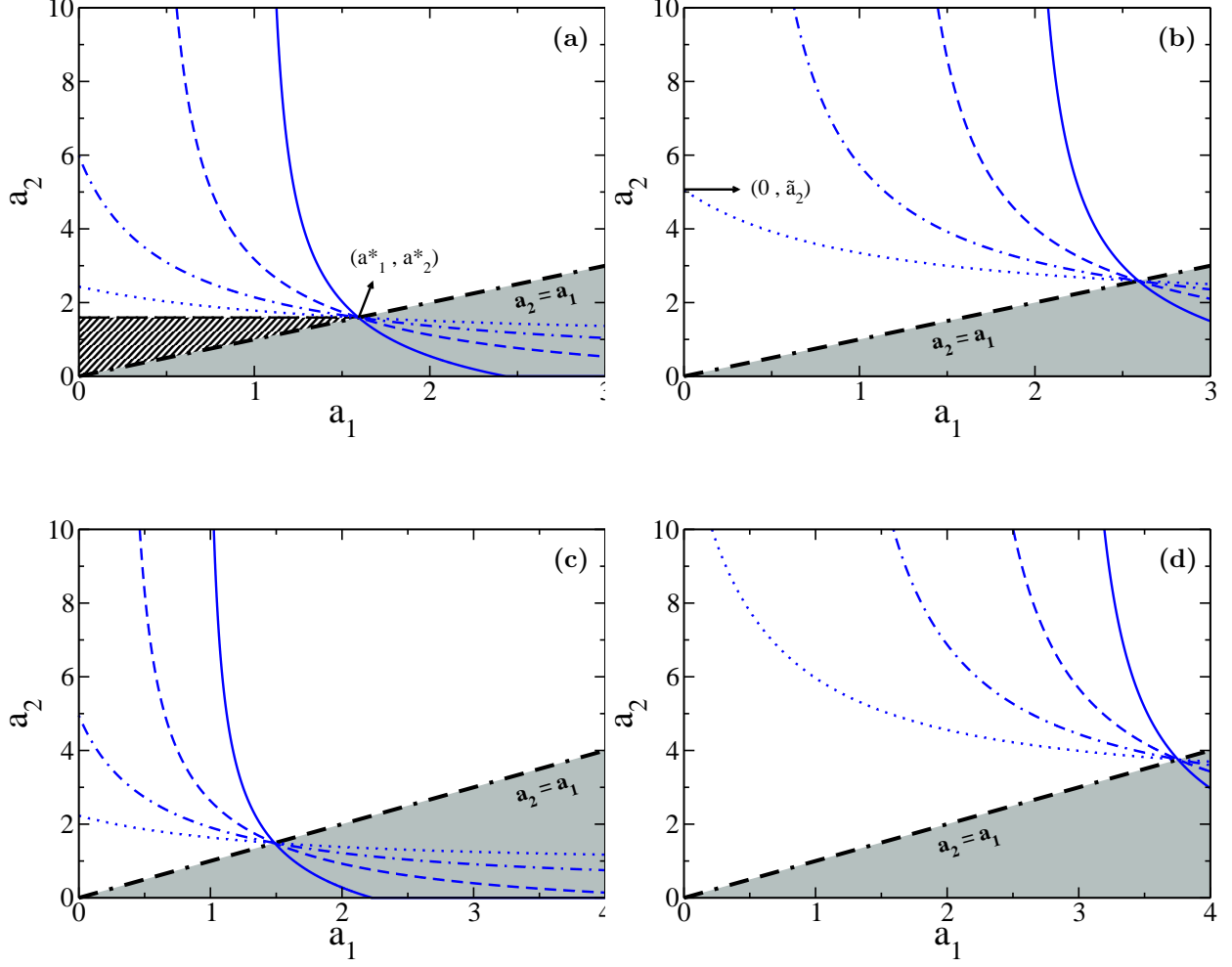


FIG. 3: Phase space of the system projected on the (a_1, a_2) plane for $t_r = 1$. Each curve represents the critical intensity a_{2c} as a function of a_1 , for different fractions of close contacts: $f_1 = 0.2$ (.....), $f_1 = 0.4$ (-.-.-), $f_1 = 0.6$ (- - -) and $f_1 = 0.8$ (—). Below each curve, the system is in an epidemic phase, while on and above is in an epidemic-free phase. Grey regions represents networks where $a_1 > a_2$, which we are not interested in. The upper figures correspond to an ER network with $\langle k \rangle = 4$, where (a) $\beta = 0.5$ and (b) $\beta = 0.7$. The lower figures represent a SF network with $\lambda = 2.5$, exponential cutoff $k_c = 50$, where (c) $\beta = 0.25$ and (d) $\beta = 0.5$. The critical values of β for a non-disordered network are $\beta_c = 0.25$ and $\beta_c \approx 0.13$, for degree distributions ER and SF with exponential cutoff respectively.

Since there is no critical value a_{2c} for $a_1 < a_{1m}$, the disease is always in an epidemic phase.

Note that there is a region of the phase space (striped region) in which the disease is in an epidemic phase for all f_1 values [see Fig. 3(a)]. This region corresponds to the epidemic phase for $f_1 = 0$, i.e., when there is only one type of contacts in the network. Then, it is characterized by $T_{a_2} > T_c = 1/(\kappa - 1)$.

We use these results to construct a distancing strategy for reducing the impact of a disease in a population with close and distant contacts, by controlling the duration of distant contact times. Suppose that the distribution of contact times has original disorder intensities a_1 and a_2 such that the system is in an epidemic phase. Then, if we assume that close contacts are a minor portion of the total ($f_1 < T_c/\beta$), we can increase the intensity a_2 to a critical point, hence reaching a non-epidemic phase independent of the original intensities [see Fig. 4(a)]. When $f_1 > T_c/\beta$, the original value of the disorder intensity of close contacts determines whether we can reach the non-epidemic phase [see Fig. 4(b)]. In this case, when $a_1 < a_{1m}$ the non-epidemic phase cannot be reached by simply increasing a_2 .

We also can observe that, if β is fixed, the critical values obtained for ER networks are lower than the ones obtained for SF networks with an exponential cutoff, as we can see comparing Figs. 3 (a) and (d). This is because in homogeneous networks (ER) individuals have, on average, the same number of neighbors. Thus, there is a limit on the speed at which the disease can be spread. In contrast, the presence of hubs in heterogeneous networks (SF) causes a rapid propagation of the disease once they become infected. Therefore, these networks require higher disorder intensities (or shorter contact times) to reach a non-epidemic phase than those required in ER networks. Note also that the intrinsic virulence of the disease β modifies these critical values.

In Figs. 3(a) and 3(b), and in Figs. 3(c) and 3(d), we show that when β increases the disease becomes more aggressive, spreads more rapidly, critical intensities increase, and the epidemic phase of the disease widens.

Finally, we generalize the analysis for larger recovery times ($t_r > 1$). In Fig. 5 we show the phase space obtained from Eqs. (1) and (2) for $t_r = 5$. This could represent the situation of a disease such as the flu, which has a mean recovery time of five days. Also, in Fig. 5 we compare these results with the $t_r = 1$ case. Note that results for different recovery times t_r do not qualitatively differ. However, for fixed f_1 , the epidemic phase becomes wider when t_r increases. This is because the infected individuals have more time to propagate the disease,

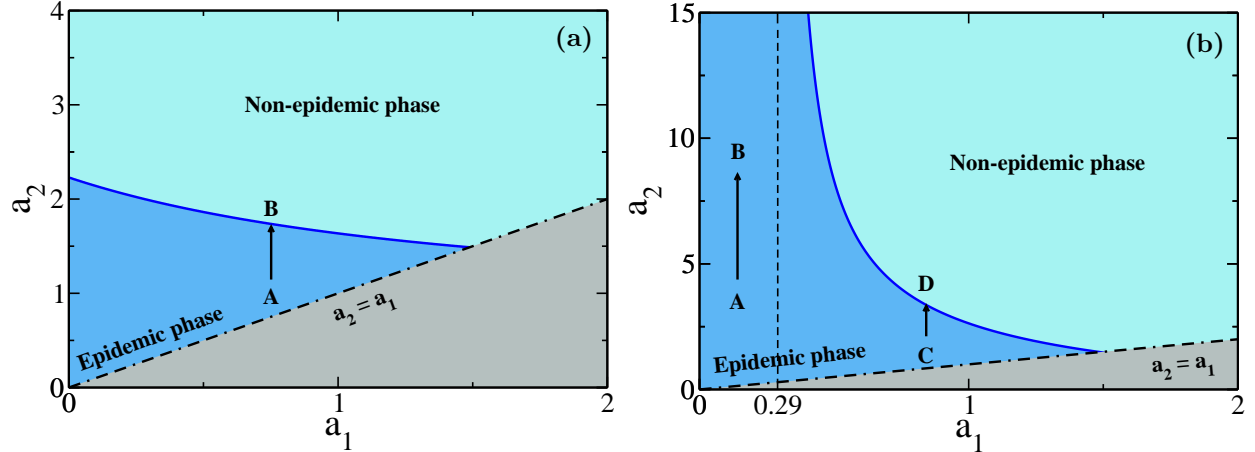


FIG. 4: Schematic of the proposed strategy to halt the spreading of a disease with virulence $\beta = 0.25$. In (a) we show the case $f_1 < T_c/\beta$ ($f_1 = 0.2$), where \tilde{a}_2 exists for $a_1 = 0$. Then, starting from any point A in the epidemic phase, by increasing a_2 we can reach the critical point in B . The opposite case is represented in (b) ($f_1 = 0.6$), which shows the same behavior than in (a) from point C to the critical point in D , for the case in which a_1 is originally greater than or equal to the minimum value a_{1m} , corresponding to $a_{2c} \rightarrow \infty$. Here $a_{1m} = 0.29$. The results correspond to a SF network with $\lambda = 2.5$ and exponential cutoff $k_c = 50$.

and thus the contact times must be shorter (or have larger disorder intensities) to move the disease to a non-epidemic phase. The recovery time is an important factor that needs to be accounted for in the implementation of our epidemic-avoiding strategy, and it varies depending on the type of disease.

IV. ANALYSIS FOR THE DISTRIBUTION $P(\omega) = 1/(a'_1\omega^{1.6})$

Some “face-to-face” experiments have studied the contact behavior of individuals at conference-like reunions. The duration of these interactions are accurately reflected by a distribution $P(\omega) \propto \omega^{-1.6}$ [1, 2]. For a more realistic analysis, we include this distribution in our model with a fraction f_1 of close contacts. We make this selection because individuals at conferences usually spend most of their time with the same group of people, a contact pattern that we define to be close. We compare our previous results with those produced by this

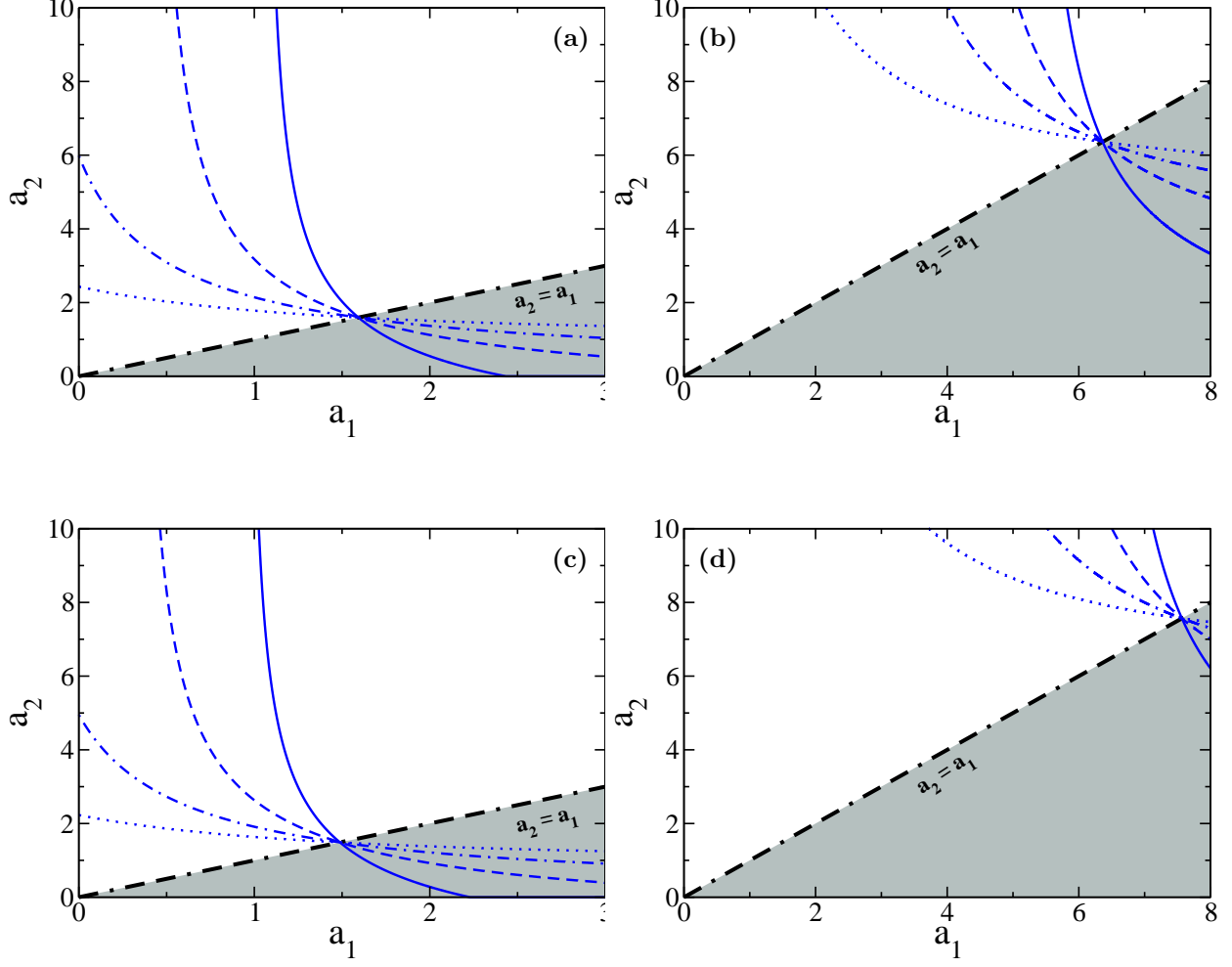


FIG. 5: Phase space of the system projected on the (a_1, a_2) plane, for different fractions of close contacts: $f_1 = 0.2$ (\cdots), $f_1 = 0.4$ ($-\cdot-$), $f_1 = 0.6$ ($- - -$) and $f_1 = 0.8$ ($—$). The upper figures correspond to an ER network with $\langle k \rangle = 4$ and $\beta = 0.5$, for (a) $t_r = 1$ and (b) $t_r = 5$. The lower figures correspond to a SF network with $\lambda = 2.5$, exponential cutoff $k_c = 50$, and $\beta = 0.25$, for (c) $t_r = 1$ and (d) $t_r = 5$. Note that the critical intensities take greater values to counter the increase of the recovery times.

new distribution, strictly defined by $P'(\omega) = 1/(a'_1\omega^{-1.6})$, where $\omega \in [(1 + 0.6a'_1)^{-5/3}, 1]$ and a'_1 is the disorder intensity.

As we stated before, now we work with a population in which a fraction f_1 of the interactions has a contact time distribution $P'(\omega) = 1/(a'_1\omega^{-1.6})$ and the fraction $f_2 = 1 - f_1$ is distributed according to $P(\omega) = 1/(a_2\omega)$. We want to compare this scenario with the

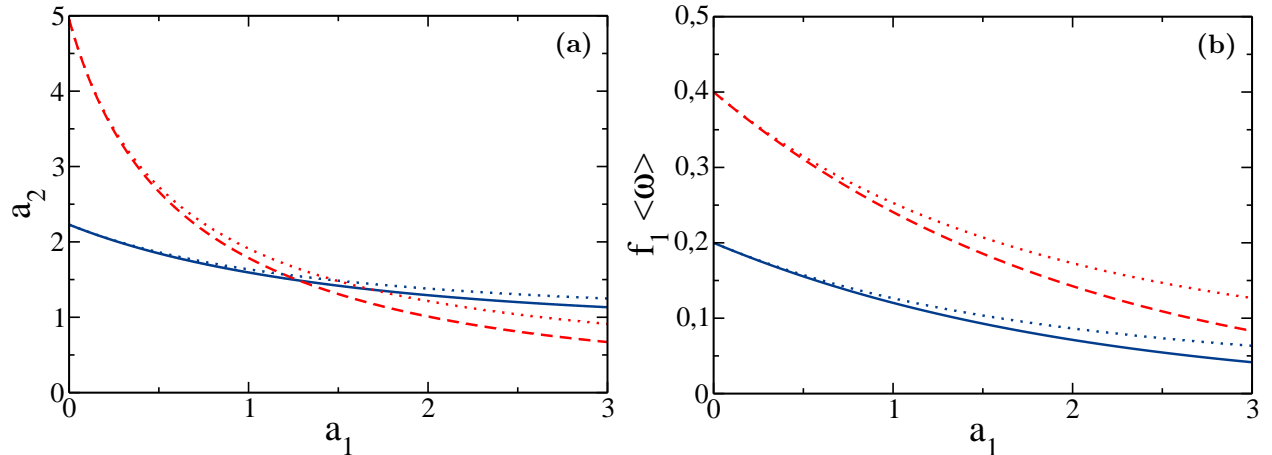


FIG. 6: (a) Critical intensities a_{2c} and (b) average normalized contact times $f_1\langle\omega\rangle$, as functions of a_1 , for different fractions of close contacts distributed according to $P'(\omega) = 1/(a'_1\omega^{-1.6})$: $f_1 = 0.2$ (—) and $f_1 = 0.4$ (- - -). The dotted lines are the corresponding results previously obtained for the distribution of close contacts $P(\omega) = 1/(a_1\omega)$. Disorder intensity a_1 is such that the minimum values of ω coincide for both distributions. Results shown in (a) correspond to a SF network with $\lambda = 2.5$, exponential cutoff $k_c = 50$, and for $\beta = 0.25$ and $t_r = 1$. Note that in (b), for a fixed value of f_1 , the difference between average contact times increases with a_1 , i.e., when the range of allowed contact times becomes wider.

previously studied case, which only differs in that the the distribution of the fraction f_1 of contact times is $P(\omega) = 1/(a_1\omega)$. In order to accurately compare these distributions, the normalized contact time ranges must be the same for both and thus, the minimum ω values must be equal. This yields $(1 + 0.6a'_1)^{-5/3} = e^{-a_1}$ and gives a relation between the disorder intensities a_1 and a'_1 . For a fixed value of a_1 , we compute the corresponding value for a'_1 and use these two intensities to obtain the critical values a_{2c} for each case. Then, we plot a_{2c} as a function of a_1 for both cases [see Fig. 6(a)]. This allows a comparison of the results when both distributions have the same range of normalized contact times. We can see that for the distribution $P'(\omega)$, the critical values a_{2c} are smaller than those that were previously obtained for $P(\omega)$, which means that the disease spreads more easily under the distribution $P(\omega)$. We can understand this if we observe Fig. 6 (b), where we show a comparison between the average normalized contact times $f_1\langle\omega\rangle'$ and $f_1\langle\omega\rangle$, corresponding

to the fraction f_1 of contacts distributed according to $P'(\omega)$ and $P(\omega)$, respectively. For any a_1 value $f_1\langle\omega\rangle' < f_1\langle\omega\rangle$, which means that the disease is less likely to propagate through interactions when the contact times are distributed according to $P'(\omega)$, the more realistic distribution of contact times that we defined from the experiments.

V. CONCLUSIONS

Using the SIR model, we studied a generalization of the disease spreading problem in disordered complex networks. We distinguished two types of network contacts, close and distant, whose presence in the system is related to the fractions f_1 and $f_2 = 1 - f_1$ respectively. Also, each type of contact is associated to an independent distribution. We focused on systems with $a_1 < a_2$, which means that close contact times are longer than those of distant contacts.

Because distant contacts are usually easier to control, we proposed a mitigation strategy that tunes the distant contacts to reduce the impact of a disease on a population. When there are only a few close contacts, this strategy can prevent the system to enter in an epidemic phase. In addition, we used a distribution of close interaction contact times that resembles the results that have been found in experiments, and we found that it is easier to reduce the impact of a disease, since it is not necessary to shorten the duration of distant interactions as much as in the previous case.

We also examined how the disease parameters affect the critical values of the disorder intensities. When the intrinsic virulence of the disease β or the recovery time t_r increase, the disease is more likely to spread across the network. As a consequence, we found that higher disorder intensities are required to prevent the emergence of an epidemic.

The analysis that we have carried out here can be taken as a first step in the study of disease propagation over disordered interconnected systems. Future research will focus on multilayer networks, in which there are individual layers or networks that interact with each other through some of their nodes. Each of these layers has its own topological properties, such as the degree distribution, and could represent different environments in which the interactions take place. We aim to study the effects of disorder in this systems, and extend the distancing strategies presented here for reducing the impact of diseases. Interconnected systems are known to accelerate these kind of spreading processes, so it is fundamental to find ways to halt them or slow them down.

ACKNOWLEDGMENTS

We acknowledge UNMdP and CONICET (PIP 00443/2014) for financial support. CELR and IAP acknowledges CONICET for financial support. Work at Boston University is supported by NSF Grants PHY-1505000, CMMI-1125290, and CHE-1213217, and by DTRA Grant HDTRA1-14-1-0017. We gratefully thank Matías A. Di Muro for useful comments.

- [1] C. Cattuto, W. V. den Broeck, A. Barrat, V. Colizza, J.-F. Pinton, and A. Vespignani, PLoS ONE **5**, e11596 (2010).
- [2] J. Stehle, A. Barrat, C. Cattuto, J. F. Pinton, L. Isella, and W. V. den Broeck, J. Theor. Biol. **271**, 166 (2011).
- [3] R. M. Anderson and R. M. May, *Infectious Diseases of Humans: Dynamics and Control* (Oxford University Press, Oxford, 1992).
- [4] N. P. A. S. Johnson and J. Mueller, Bull. Hist. Med. **76**, 105 (2002).
- [5] C. Fraser, C. A. Donnelly, S. Cauchemez, W. P. Hanage, M. D. Van Kerkhove, T. D. Hollingsworth, J. Griffin, R. F. Baggaley, H. E. Jenkins, E. J. Lyons, *et al.*, Science **324**, 1557 (2009).
- [6] S. Merler, M. Ajelli, L. Fumanelli, M. F. C. Gomes, A. Pastore y Piontti, L. Rossi, D. L. Chao, I. M. Longini, M. E. Halloran, and A. Vespignani, Lancet Infect. Dis. **15**, 204 (2015).
- [7] N. . M. Fox, “New york is fighting its worst outbreak of measles in decades,” (2019).
- [8] A. E. van den Bogaard and E. E. Stobberingh, Int. J. Antimicrob. Ag. **14**, 327 (2000).
- [9] World Health Organization, “Using climate to predict infectious disease outbreaks: A review,” (2004).
- [10] A. J. McMichael, R. E. Woodruff, and S. Hales, The Lancet **367**, 859 (2006).
- [11] M. Greger, Crit. Rev. Microbiol. **33**, 243 (2007).
- [12] M. E. J. Newman, Phys. Rev.E **66**, 016128 (2002).
- [13] S. Boccaletti, V. Latora, Y. Moreno, M. Chavez, and D. Hwang, Phys. Rep. **424**, 175 (2006).
- [14] M. E. J. Newman, *Networks: An Introduction* (Oxford University Press, 2010).
- [15] C. Castellano and R. Pastor-Satorras, Phys. Rev. Lett **105**, 218701 (2010).

- [16] R. Pastor-Satorras, C. Castellano, P. Van Mieghem, and A. Vespignani, *Rev. Mod. Phys.* **87**, 925 (2015).
- [17] W. Wang, M. Tang, H. E. Stanley, and L. A. Braunstein, *Reports on Progress in Physics* **80**, 036603 (2017).
- [18] P. Grassberger, *Math. Biosci.* **63**, 157 (1983).
- [19] N. T. J. Bailey, *The Mathematical Theory of Infectious Diseases* (Griffin, London, 1975).
- [20] J. C. Miller, *Phys. Rev. E* **76**, 010101 (2007).
- [21] E. Kenah and J. M. Robins, *Phys. Rev. E* **76**, 036113 (2007).
- [22] C. Lagorio, M. V. Migueles, L. A. Braunstein, E. López, and P. Macri, *Physica A* **388**, 755 (2009).
- [23] L. A. Meyers, *Bull. Amer. Math. Soc.* **44**, 63 (2007).
- [24] M. J. Ferrari, S. Bansal, L. A. Meyers, and O. N. Bjørnstad, *Proc. R. Soc. London, Ser. B* **273**, 2743 (2006).
- [25] S. Bansal, B. Pourbohloul, and L. A. Meyers, *PLoS Med.* **3**, e387 (2006).
- [26] M. A. Di Muro, L. G. Alvarez-Zuzek, S. Havlin, and L. A. Braunstein, *New J. Phys.* **20**, 083025 (2018).
- [27] T. Gross, C. J. Dommar D’Lima, and B. Blasius, *Phys. Rev. Lett.* **96**, 208701 (2006).
- [28] C. Lagorio, M. Dickison, F. Vazquez, L. A. Braunstein, P. A. Macri, M. V. Migueles, S. Havlin, and H. E. Stanley, *Phys. Rev. E* **83**, 026102 (2011).
- [29] C. Buono, C. Lagorio, P. A. Macri, and L. A. Braunstein, *Physica A* **391**, 4181 (2012).
- [30] L. D. Valdez, P. A. Macri, and L. A. Braunstein, *Phys. Rev. E* **85**, 036108 (2012).
- [31] C. Buono, F. Vazquez, P. A. Macri, and L. A. Braunstein, *Phys. Rev. E* **88**, 022813 (2013).
- [32] K. Eastwood, D. N. Durrheim, M. Butler, and E. Jon, *Emerg. Infect. Dis.* **16**, 1211 (2010).
- [33] M. Karsai, M. Kivelä, R. K. Pan, K. Kaski, J. Kertész, A.-L. Barabási, and J. Saramäki, *Phys. Rev. E* **83**, 025102 (2011).
- [34] L. D. Valdez, C. Buono, P. A. Macri, and L. A. Braunstein, *FRACTALS* **21**, 1350019 (2013).
- [35] M. Molloy and B. Reed, *Random Struct. Algor.* **6**, 161 (1995).
- [36] L. A. Braunstein, Z. Wu, Y. Chen, S. V. Buldyrev, T. Kalisy, S. Sreenivasan, R. Cohen, E. Lpez, S. Havlin, and H. E. Stanley, *International Journal of Bifurcation and Chaos* **17**, 2215 (2007).
- [37] M. E. J. Newman, S. H. Strogatz, and D. J. Watts, *Phys. Rev. E* **64**, 026118 (2001).

[38] M. E. J. Newman, *SIAM Rev.* **45**, 167 (2003).